Journal of NeuroVirology, 8: 318–325, 2002
 ISSN 1355–0284/02 $12.00+.00
DOI: 10.1080/13550280290100699

The peroxisome proliferator phenylbutyric acid (PBA) protects astrocytes from *ts*1 MoMuLV-induced oxidative cell death

Na Liu,[1] Wenan Qiang,[1] Xianghong Kuang, Philippe Thuillier, William S Lynn, and Paul KY Wong*

University of Texas, M.D. Anderson Cancer Center, Science Park—Research Division, Smithville, Texas, USA

Oxidative stress is involved in the pathogenesis of several neurodegenerative diseases, including Parkinson's disease, Alzheimer's disease, and HIV neuroAIDS. In this study, we have investigated an agent, phenylbutyric acid, that ameliorates cell death in murine astrocytes infected with *ts*1 MoMuLV (*ts*1). Phenylbutyric acid, an aromatic short chain fatty acid, was shown to prevent the loss of catalase that occurs in *ts*1 infected astrocytes, and to prevent *ts*1-mediated cell death. Cell cotransfection studies demonstrated that phenylbutyric acid activates peroxisome proliferator receptors (PPARs) in astrocytes, and binds to the peroxisome proliferator-activated receptors α and γ. This observation suggests that the effects of PBA may be mediated by PPARs in astrocytes. Phenylbutyric acid also maintained catalase protein levels in brain of *ts*1-infected mice, and delayed the hindlimb paralysis caused by *ts*1 infection. Because PBA activates peroxisome proliferator-activated receptors and prevents loss of catalase, we suggest that *ts*1-induced oxidative stress in infected astrocytes that is alleviated by PBA is mediated via PPARα and/or PPARγ. *Journal of NeuroVirology* (2002) **8,** 318–325.

Keywords: retrovirus-induced neurodegeneration; peroxisome proliferator-activated receptors; catalase; phenylbutyric acid

Introduction

The retrovirus *ts*1, a mutant of Moloney murine leukemia virus (MoMuLV), causes a progressive neuroimmunodegenerative syndrome in FVB/N mice that have been infected with the virus within the first few days after birth [reviewed in (Wong *et al*, 1998)]. Infection of the central nervous system by this route results in neuronal loss with gliosis and spongiform lesions without inflammatory cell infiltration (Stoica *et al*, 1993; Stoica *et al*, 2000). The infected cells include astrocytes, microglia, and oligodendrocytes, but not neurons (Stoica *et al*, 1993). These histopathological features are similar to those observed in brains of humans infected with HIV (Stoica *et al*, 1993; Stoica *et al*, 2000).

Astrocytes are known to be required for survival of neurons during perinatal development (Ullian *et al*, 2001) and during postnatal stress (Miele *et al*, 1994; Takeshima *et al*, 1994). Infection of astrocytes by *ts*1 during neuronal development, with loss of support functions for neurons may be responsible for the neurodegeneration seen in *ts*1 infected mice. Earlier studies from this laboratory showed that *ts*1 envelope proteins accumulate in the endoplasmic reticulum (ER) in infected astrocytes (Shikova *et al*, 1993; Stoica *et al*, 1993). In primary astrocyte cultures and in astrocytic cell lines, this accumulation of envelope proteins is accompanied by profound cytopathic

*Address correspondence to Paul KY Wong, University of Texas, M.D. Anderson Cancer Center, Science Park—Research Division, P.O. Box 389, Smithville, TX 78957, USA. E-mail: pwong@sprd1.mdacc.tmc.edu

We thank Sarah Henninger for her assistance in preparing the manuscript and Yu Liu for technical assistance. We are also most grateful to Drs Dean Tang and Virginia Scofield for their critical reviews of the manuscript. In addition, we thank Dr Steven A Kliewer for providing pSG5-GAL4-PPARα, pSG5-GAL4-PPARβ, pSG5-GAL4-PPARγ, pMH-100-TK Luciferase reporter, and PPRE$_3$-TK-Luciferase reporter plasmids. We also thank Dr Jack Vanden Heuvel for providing pSG5-PPARβ plasmid. This work was supported by NIH grants AI28283, MH57181, and NIEHS (Center Grant ES07784).

[1]Equal contributions by these authors.

Received 24 January 2002; revised 1 April 2002; accepted 1 May 2002.

effects (Shikova *et al*, 1993; Lin *et al*, 1997). We hypothesized that this accumulation of envelope proteins in ER activates an ER overload response, resulting in elevated intracellular production of reactive oxygen species (ROS) (Pahl and Baeuerle, 1997; Rizzuto *et al*, 1998; Hacki *et al*, 2000). We further hypothesized that the increased ROS activate apoptotic pathways in astrocytes, depriving neurons of astrocytic support and releasing astrocyte-derived neurotoxins, thereby triggering neuronal dysfunction and death.

Peroxisome proliferator activated receptors (PPARs) are members of a large nuclear hormone receptor superfamily. Activation of PPARs by their ligands, such as peroxisome proliferators or fatty acids, causes the PPARs to heterodimerize with the retinoid X receptor (RXR), allowing binding of the complex to DNA on PPRE, and resulting in transcriptional activation of target genes (Kliewer *et al*, 1992). Ligand-activated PPARs have been shown to play roles in lipid homeostasis, adipocyte differentiation, inflammation, and carcinogenesis (Gelman *et al*, 1999; Escher and Wahli, 2000). PPARα activation results in the transcriptional upregulation of many genes, including those involved in β-oxidation and antioxidant enzymes (e.g., catalase). It is generally known that while the H_2O_2 generating enzymes, e.g., acyl-CoA oxidase, are induced 20- to 40-fold by peroxisome proliferators in the liver, there is only a moderate 2-fold increase in catalase activity (Reddy *et al*, 1986; Yeldandi *et al*, 2000). However, it is not likely that the imbalance between the H_2O_2-generating enzymes and H_2O_2-degrading enzymes after peroxisome proliferator treatment reflects the oxidative states of the cells (Handler *et al*, 1992; Soliman *et al*, 1997). It has been shown that engagement of ligand-activated PPARα receptor modulates cellular redox status and alleviates oxidative damage in splenocytes and hepatocytes, by upregulating antioxidants, such as catalase, ubiquinone, and superoxide dismutase (Inoue *et al*, 1998; Poynter and Daynes, 1998). PPARs have also been detected in the brain, but their functions there are not well defined.

The short-chain fatty acid phenylbutyric acid (PBA) (Figure 1) was identified originally as a suppressor of tumor cell growth (Samid *et al*, 1993; DiGiuseppe *et al*, 1999). Recent work has shown that PBA is a potent PPARγ ligand (Samid *et al*, 2000). We report here that PBA prevents both the loss of catalase and the death of *ts*1-infected astrocytes. We also show that PBA activates PPARs in astrocytes, and binds to the PPARα and PPARγ. Finally, we show that treatment of *ts*1-infected mice with PBA prevents loss of catalase in the infected brain and delays hindlimb paralysis. Together our results suggest that PBA protects *ts*1-infected astrocytes against virus-induced oxidative stress by binding to PPARs, thereby maintaining levels of antioxidant enzymes such as catalase. PBA or other PPARα ligands thus may become therapeutically useful in *ts*1-mediated neurodegeneration, and possibly in other neurodegenerative diseases that involve oxidant damage in glial cells.

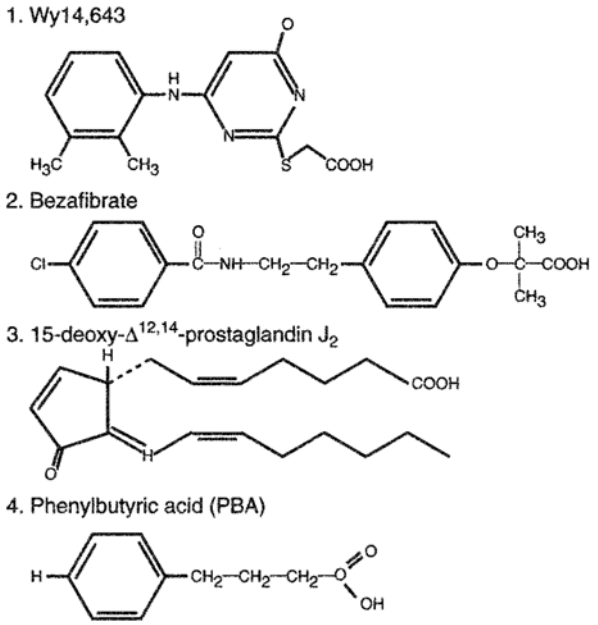

Figure 1 Chemical structures of PBA and other known PPAR ligands. (**1**) Wy 14,643. (**2**) Bezafibrate. (**3**) 15-deoxy-$\Delta^{12,14}$ prostaglandin J2. (**4**) Phenylbutyric acid (PBA).

Results

PBA rescues astrocytes from ts*1-induced cell death*

Figure 2A shows that PBA prevents death of C1 cells after *ts*1 infection. At 72 h after infection, numbers of viable cells in *ts*1-infected C1 cells were significantly decreased relative to control uninfected C1 cells. This cell loss was prevented if PBA (75 μg/ml) was present in the culture medium. MTS assays for cell viability also demonstrated that cell death induced by *ts*1 is prevented by PBA (Figure 2B).

PBA prevents catalase depletion in ts*1-infected C1 astrocytes*

To determine whether PBA prevents catalase depletion in *ts*1-infected C1 astrocytes, catalase protein levels were assayed by Western blotting over time after infection. Figure 3 shows that while cells from control infected cultures showed a steep decline in catalase levels by 48–72 h postinfection (p.i.), catalase levels were maintained through this interval, at close-to-normal levels, in cells of cultures treated with PBA.

PBA activates PPARs in astrocytic cell lines

To determine whether PBA treatment activates PPARs in cultured astrocytes, we examined the effect of PBA on the activity of a transfected PPRE linked to a luciferase reporter plasmid. As shown in Figure 4,

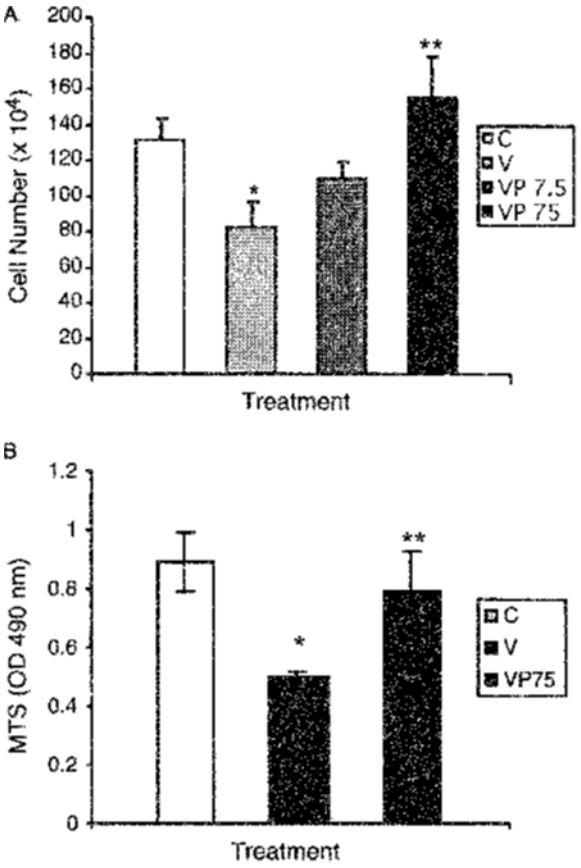

Figure 2 Effects of PBA on *ts*1-infected C1 cells. (**A**) Cell viability measured by cell counts. (**B**) Cell viability measured by MTS colorimetric assay. Then, 7.5 and/or 75 μg/ml of PBA was added to the cultures after *ts*1 infection for 72 h. C, Uninfected C1 cells, V, *ts*1-infected C1 cells, VP7.5, *ts*1-infected cells treated with 7.5 μg/ml PBA, VP75, *ts*1-infected C1 cells treated with 75 μg/ml PBA. Data were expressed as the mean ± SD of results of quintuplicate cultures. Statistical significance was compared between C and V or between V and VP75 separately. $^{*}P < 0.01$ *versus* C, $^{**}P < 0.01$ *versus* V. The results represent three separate experiments.

transfected C1, C6, and primary cortical astrocyte (PCA) cell cultures all showed significantly increased luciferase activities when treated with 75 μg/ml PBA.

PBA binds both PPARα and PPARγ, but not PPARβ

Because PBA activates PPARs and affects the expression of the peroxisome-containing enzyme catalase, we inferred that PBA might bind directly to PPARs. We therefore tested the ability of PBA to bind specifically to particular PPAR isoforms, using a chimeric receptor/reporter system in which the ligand-binding domain of PPARα, β, or γ is fused to the DNA binding domain of the yeast transcription factor Gal 4. The chimeric receptor binds to the Gal 4 binding motif, but activates transcription only in response to engagement of the ligand-binding domain (LBD) of the PPAR (Forman *et al*, 1995). Figure 5 shows that in C6 cells, PBA binds directly to two of the three PPAR isoforms (PPARα and PPARγ), but that it binds with notably greater affinity to PPARα than to PPARγ.

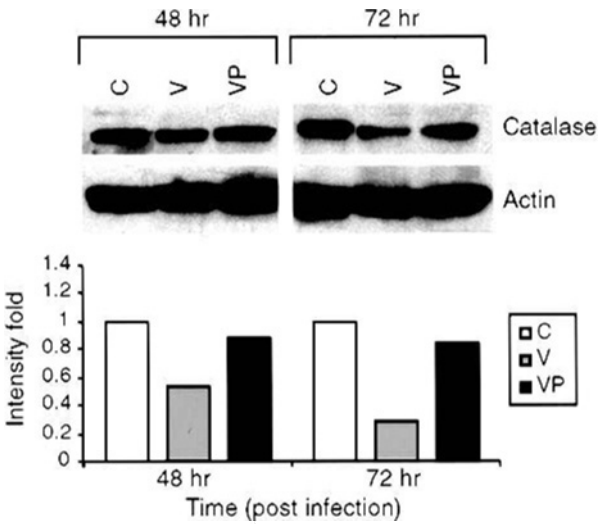

Figure 3 Effects of PBA on catalase protein levels in *ts*1-infected C1 cells. C1 cells were infected with *ts*1 at a MOI of 4 for 40 min in 100-mm dishes, and 75 μg/ml PBA was added immediately following infection. C, uninfected C1 cells, V, *ts*1-infected C1 cells, VP, *ts*1-infected C1 cells treated with PBA. After imaging, the same blots were stripped and immunoblotted with anti-actin antibody. Intensity of catalase protein expression is normalized to actin loading in each plot ($n = 3$). Results are expressed as intensity-fold relative to control cells (set at a value of 1). Blots shown are representative of two independent experiments.

At 100 μg/ml, PBA induced PPARα activation by 60-fold, whereas it only induced PPARγ activation by only 2-fold. In the same cells, the PPARβ ligand bezafibrate bound strongly to PPARβ, indicating that PBA did not bind the LBD of PPARβ. These results further support the idea that the preventive role of PBA in *ts*1-induced death is mediated in part through PPARs, particularly via PPARα. Similar binding

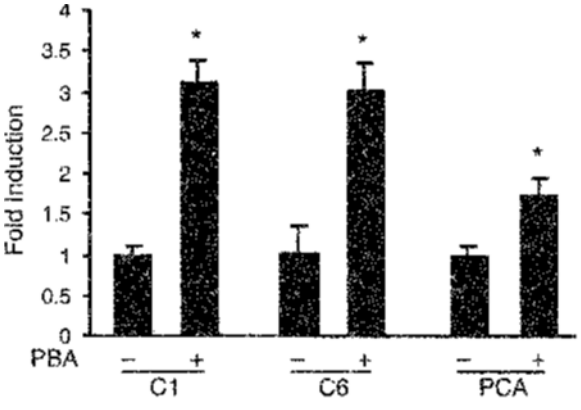

Figure 4 Effects of PBA on $PPRE_3$-TK-luc activity in cultured C1, C6, or PCA cells. Cotransfection of $PPRE_3$-TK-luc and CMV-β-gal was performed as described in Materials and methods. 75 μg/ml PBA was added to the wells following transfection. After 24 h for C1 or C6 cells, and 48 h for PCA cells, the cells were lysed and harvested for luciferase and β-gal assays, as described in Materials and methods. The data shown represent luciferase activity normalized with β-gal. Results are expressed as fold-activation relative to control cells (represented as 1). Each experiment was repeated at least three times, with similar results. $^{*}P < 0.01$ *versus* PBA-untreated control cells.

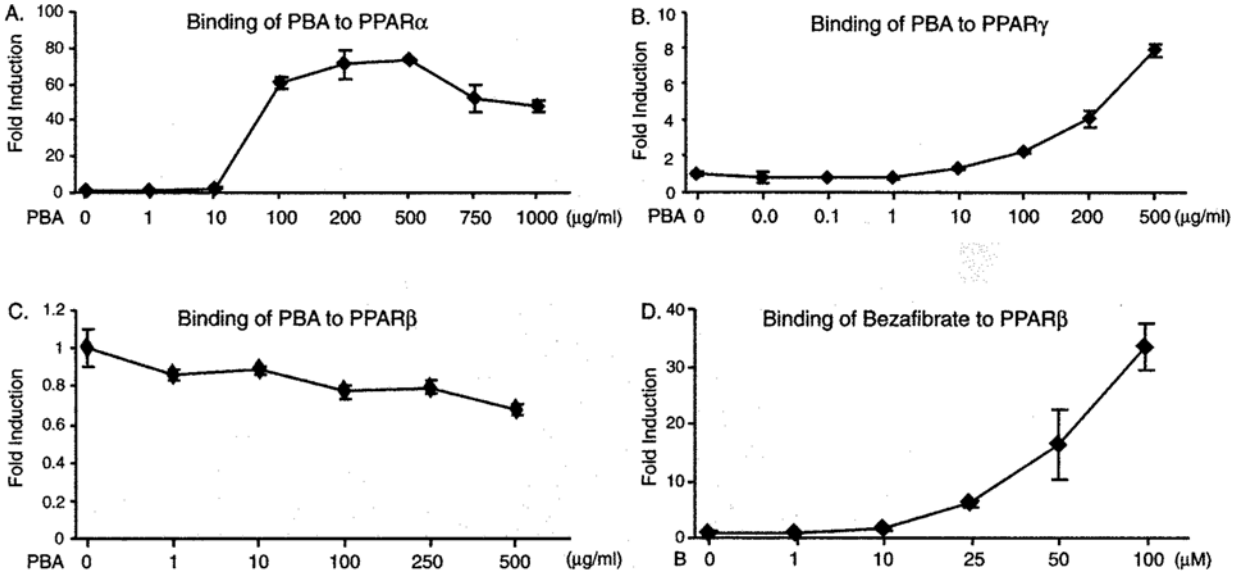

Figure 5 Ligand binding domain activation of PPARs in C6 cells. Cotransfection of pSG5-GAL4-PPARs, pMH-100-Tk-Luciferase, and CMV-β-gal was performed as described in Materials and methods. Different concentrations of PBA or other ligands were added to the wells following transfection. After 24 h, the cells were lysed and harvested for luciferase and β-gal assays, as described in Materials and methods. (**A**) Binding of PBA to PPARα LBD. (**B**) Binding of PBA of PPARγ LBD. (**C**) Binding of PBA to PPARβ LBD. (**D**) Binding of bezafibrate to PPARβ LBD. Binding of known ligands to PPARα and PPARγ is not shown here. The data shown represent luciferase activity normalized with β-gal. Results (means $\pm$ SD) are expressed as fold-activation relative to control cells (represented as 1). Each experiment was repeated three times with similar results.

results were obtained in C1 and PCA cells (data not shown).

PBA delays ts*1-induced hindlimb paralysis and prevents loss of catalase in* ts*1-infected brain stem in tissue of FVB/N mice*

As shown in Figure 6, the incidence of hindlimb paralysis was 100% by 43 days after infection in control mice ($n = 16$). Hindlimb paralysis was significantly delayed in infected animals treated with PBA ($n = 8$). In the same animals, brain stem catalase levels did not decline in PBA-treated infected mice (Figure 7).

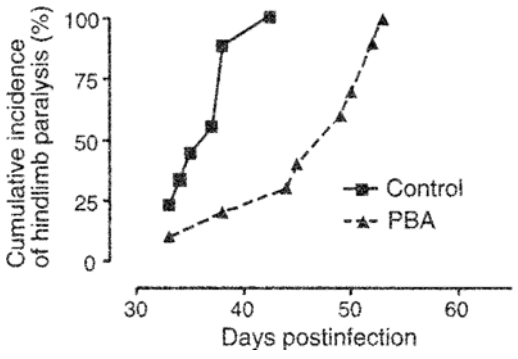

Figure 6 Effect of PBA on hindlimb paralysis of *ts*1-infected mice. Newborn FVB/N pups were injected intraperitoneally with *ts*1. Then, 750 mg/kg PBA was administered intraperitoneally to the *ts*1-infected pups at 5 days p.i. and daily thereafter. The same amount of saline was given to *ts*1 infected and uninfected mice as a control. The cumulative incidence of hindlimb paralysis for PBA-treated and untreated *ts*1-infected mice is shown. The difference between PBA ($n = 8$) and the saline control group ($n = 16$) is significant ($P < 0.01$).

Discussion

Oxidative stress causes the depletion of endogenous antioxidants, such as superoxide dismutase (SOD), glutathione (GSH), and catalase, thereby increasing production of ROS (Pace and Leaf, 1995). It is well known that neural tissue is especially sensitive to

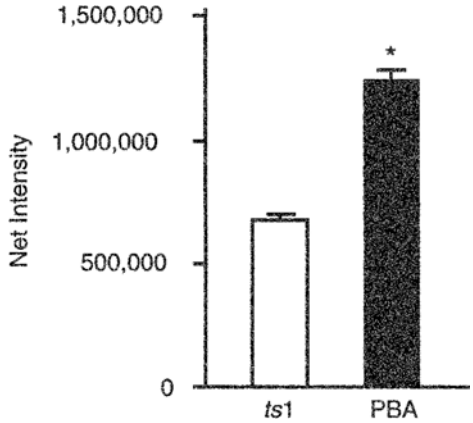

Figure 7 Effect of PBA on brain stem catalase. Mice were sacrificed and 50 μg protein extract from the brain stem of each mouse used for Western blotting analysis. The blots were scanned and analyzed at a Kodak image station. Intensity-fold of catalase expression, normalized by actin loading in each plot, is indicated by the graph. *ts*1, *ts*1-infected mice ($n = 16$); PBA, *ts*1-infected mice treated with 750 mg/kg PBA ($n = 8$). $^*P < 0.01$ *versus ts*1 group.

oxidative stress, and oxidant stress has been identified as a prominent factor in acute and chronic neurodegenerative diseases and in traumatic brain insults. Therapeutic strategies centered on antioxidants and on free-radical scavengers have therefore been proposed for treatment of several brain pathologies. Oxidative stress has been implicated in the pathogenesis of neuroAIDS (Mollace *et al*, 2001).

*ts*1 infection in mice shares some common characteristics with HIV infection in humans. In *ts*1-infected mice, as in HIV-infected humans, there is selective depletion of $CD4^+$ T cells, thymocytes, and neurons. In the nervous system, as in neuroAIDS, an inflammatory response and ROS-mediated damage occur. Glial cells, but not neurons, are infected by both viruses (Stoica *et al*, 1993; Stoica *et al*, 2000); thus, the neuropathogenic effects of *ts*1, like those of HIV, are not due to direct infection of neurons.

Neurons must reduce large amounts of O_2 to maintain neurotransmission, and so they produce particularly large amounts of ROS. For this and other reasons, neurons are more vulnerable than other cell types to oxidative stress. Neurons are dependent on astrocytes for their supply of thiol and redox support (Dringen *et al*, 1999), which are especially necessary for these cells due to their high vulnerability to oxidant stress. Loss of this astrocytic redox support function may lead to neuronal death. We show here that *ts*1-infected astrocytes are under oxidative stress, made evident by reduction of catalase levels. After *ts*1 infection, cultured astrocytes fail to provide cysteine for neuronal glutathione synthesis (unpublished data), and they increase their production of cytokines, particularly IL-6 (unpublished data). The expression of TNFα, IL-1 (Choe *et al*, 1998), and iNOS (Kim *et al*, 2001) are also induced in *ts*1-infected astrocyte cultures. Together these data indicate that *ts*1-infected astrocytes are not able to provide normal redox support to neurons, and that they also trigger inflammatory processes proximal to neurons. Both could contribute to neuronal death in this neurodegenerative damage after *ts*1 infection.

We have found that PBA is a ligand for PPARα, and to a lesser extent, for PPARγ, but not for PPARβ. This is consistent with the recent observation that short chain fatty acids, such as PBA, bind selectively to PPARα (Johnson *et al*, 1997). PPARs have been shown recently to be expressed in the central nervous system (Cullingford *et al*, 1998). Both neurons and astrocytes contain high mRNA levels of PPARs, especially PPARβ (Cullingford *et al*, 1998), but the functions of PPARs in the central nervous system are poorly understood. Our data show that the PPARα activator PBA, prevents *ts*1-mediated cell death. This finding directly implicates PPARs in prevention of *ts*1-mediated astrocytic cell death.

In a recent report (Poynter and Daynes, 1998), PPARα transcripts and catalase levels were shown to be reduced in the splenocytes of old animals, but were restored when the mice were treated with PPARα activators. In the same study, the elevated lipid peroxidation normally seen in older splenocytes was also attenuated by PPARα activators. Because membrane lipid peroxidation is an endpoint marker of cellular oxidant stress, its reduction in response to PPARα activators could be taken to reflect a net restoration in cellular redox balance.

Because PBA delays *ts*1-induced hindlimb paralysis, and upregulates catalase, we suggest that the protective effect of PBA in mice may be mediated, at least in part, by activating PPARα and maintaining catalase. Activation of PPARα, and PPARγ has also been demonstrated to reduce inflammatory responses and to alleviate oxidative damage, by modulating redox-regulated transcription factor nuclear factor-κB (NF-κB), (Poynter and Daynes, 1998), and by inhibiting proinflammatory factors and cytokines, such as TNFα and IL-6 (Combs *et al*, 2001). Cell survival is therefore likely to be a net effect resulting from multiple intracellular consequences of PBA treatment. Because *ts*1-induced neurodegenerative damage is a result of multiple mechanisms, we propose that PBA, and other PPARα agonists, may maintain redox balance in astrocytes, and/or inhibit their production of inflammatory mediators, thereby improving glial support of neurons. If so, PBA, PPARα agonists, and other agents that maintain redox balance, may prove to be therapeutically useful for treatment of virus-induced neurodegenerative syndromes.

Materials and methods

Animal treatment

Newborn pups were infected intraperitoneally with *ts*1. The titre of all *ts*1 used in this study was 1.7×10^7 infectious unit/ml. PBA was dissolved by sterilized saline water. Administration of 750 mg/kg PBA was started as early as 5 days p.i. and was repeated daily thereafter. Hindlimb paralysis was monitored in PBA-treated ($n = 8$), untreated *ts*1-infected (saline control, $n = 16$) mice and uninfected controls ($n = 8$). Treated pups within individual experiments were from the same litter.

Astrocyte preparation

Primary cortical astrocytes were isolated from 1- to 2-day-old FVB mice by a modification of methods described previously (Shikova *et al*, 1993). The cells were plated onto poly-L-lysine-coated flasks and grown in DMEM/F-12 medium supplemented with 10% FBS, 100 U/ml penicillin, 100 μg/ml streptomycin, and 2.5 μg/ml fungizone for 7 to 9 days, until reaching confluence. The cells were then passaged 4 to 5 times before use. These cultures contained more than 85% glial fibrillary acidic protein (GFAP)-positive cells, as detected using rabbit anti-mouse GFAP antibody (DAKO Corp., Carpinteria, CA, USA). The mouse C1 cell line was obtained by immortalizing primary astrocytes with SV-40

large T antigens. The C6 line is a rat glial cell line purchased from the American Type Culture Collection (ATCC). C1 and C6 cells were grown in DMEM medium supplemented with 10% FBS, 100 U/ml penicillin, and 100 μg/ml streptomycin at 37°C in a humidified atmosphere of 5% CO_2 in air.

ts1 infection of C1 cells and treatment

C1 cells were seeded in 60-mm or 100-mm plastic tissue culture dishes and incubated overnight in DMEM medium containing 1% FBS and 3 μg/ml polybrene, to enhance viral absorption. The next day, the cells were infected with *ts*1 for 40 min at a multiplicity of infection (MOI) of 4 (in DMEM medium containing polybrene, as before). The cells were then washed and re-fed with fresh DMEM medium with 5% FBS, either with or without treatment with PBA. The treated and control cultures were incubated at 37°C and harvested at 48 and 72 h p.i. for cell counts or for Western blot analysis of protein levels.

Cell number and viability assay

For all cultures, cell viability and cell numbers were determined daily after *ts*1 infection. The cultures were trypsinized and cell suspensions stained with trypan blue for 10 min prior to counting.

Cell viability and growth were also followed using the redox-sensitive tetrazolium salt assay kit. This assay is based on the bioreduction of MTS, 3-(4,5-dimethylthiazol-2-7)-5-(3-carboxymethoxyphenyl)-2-(4-sulfophenyl)-2H-tetrazolium to a colored formazan as described (Goodwin *et al*, 1995). MTS assays were performed using Cell Titer 96 Aqueous One Solution Reagent (Promega, USA), according to the manufacturer's instructions. Cells were plated in 96-well plates at 3×10^4 cells in a volume of 100 μl/well. Then, 20 μl of the preceding reagent was added into each well at 24, 48, and 72 h p.i. After 2 h of incubation at 37°C in a humidified 5% CO_2 atmosphere, absorbance at 490 nm was recorded using a 96-well plate reader (Spectra Count, Packard). Cell count and MTS assay were carried out quintuplicate and repeated three times.

Western blot analysis

Total cellular or tissue proteins were isolated using RIPA buffer (1% NP40, 0.5% sodium deoxycholate, 0.1% SDS, 0.25 mM PMSF, 1 μg/ml aprotinin, leupeptin, and pepstatin, 1 mM sodium orthovanadate, and 1 mM sodium fluoride in PBS) as described (Thuillier *et al*, 1998). Protein concentrations were measured using Bio-Rad D_C protein Assay Reagent (BioRad Laboratories, Hercules, CA, USA) following the manufacturer's instructions. For catalase, the lysates (50 μg total protein per sample) were electrophoresed on 10% SDS-PAGE gels. After electrophoresis, the resolved proteins were transferred to PVDF membranes (Millipore Corp, Bedford, MA, USA). The membranes were blocked for 1 h in TBS with 5% nonfat milk at room temperature, and subsequently immunoblotted with anti-catalase antibody (Rockland, Inc, Gilbertsville, PA) and washed. After reaction with horseradish peroxidase-conjugated goat anti-rabbit IgG (TAGO Immunologicals, Camarillo, CA, USA), immune complexes were detected using a chemiluminescent reagent (NEN Life Science Products, Inc, Boston, MA, USA). A monoclonal anti-actin antibody (Oncogene Research Products, Boston, MA, USA) was used as a control for protein loading. The same Western blotting analysis was performed in two independent experiments.

Reporter assays

Cotransfections were performed as described previously (Thuillier *et al*, 2000). C1, C6, and PCA cells were seeded into 6-well plates at a concentration of 2×10^5 cells/well, and then transfected with plasmids the next day. All transfections were done using FuGENE6 transfection reagent (Roche Diagnostics Corp, Indianapolis, IN, USA).

For determination of PPAR activation, cells were transfected with 0.875 μg of the $PPRE_3$-TK-luc reporter plasmid (kindly provided by Dr Steven A Kliewer, Glaxo Wellcome), and 0.125 μg CMV-β-galactosidase plasmid (CMV-β-gal) in a volume of 100 μl/well.

Transfections to study PPAR ligand binding domain activity were done as previously described (Muga *et al*, 2000), using 0.5 μg pSG5-GAL4-PPARα, pSG5-GAL4-PPARβ, or pSG5-GAL4-PPARγ, with 0.5 μg pMH-100-TK-Luciferase reporter (donated by Dr Steven A Kliewer), combined with 0.125 μg CMV-β-gal in a volume of 100 μl/well. Ligands and PBA were added to the wells following transfection. Ligands used as controls were Wy14, 643 for PPARα, bezafibrate for PPARβ and 15-deoxy-$\Delta^{12,14}$-prostaglandin J2 for PPARγ (Figure 1). Wy14,643 was dissolved in distilled water, bezafibrate in ethanol, and 15-deoxy-$\Delta^{12,14}$-prostaglandin J2 was dissolved in DMSO, aliquoted, and sealed by nitrogen. The different solvents were used as control inocula in transfection assays according to the ligand tested.

After 24 h for C1 or C6, or 48 h for PCA, cells were lysed for luciferase and β-gal activity assays. Luciferase activity was measured using a luciferase assay reagent (Promega Corp, Madison, WI, USA). β-Gal assays were performed using Galactolight kit in a luminometer (Gen-PROBE). Each transfection was carried out in triplicate and repeated at least three times.

Statistical analysis

Data are presented as mean ± SD. The statistical significance of results was determined by Student's *t*-test. The cumulative incidence of hindlimb paralysis in infected mice was determined by analysis of covariance comparing slopes for *ts*1-infected mice to those *ts*1-infected mice treated with PBA.

References

Choe WK, Stoica G, Lynn WS, Wong PKY (1998). Neurodegeneration induced by MoMuLV-*ts*1 and increased expression of TNFα and Fas in the central nervous system. *Brain Res* **779:** 1–8.

Combs CK, Bates P, Karlo JC, Landreth GE (2001). Regulation of beta-amyloid stimulated proinflammatory responses by peroxisome proliferator-activated receptor alpha. *Neurochem Int* **39:** 449–457.

Cullingford TE, Bhakoo K, Peuchen S, Dolphin CT, Patel R, Clark JB (1998). Distribution of mRNAs encoding the peroxisome proliferator-activated receptor alpha, beta, and gamma and the retinoid X receptor alpha, beta, and gamma in rat central nervous system. *J Neurochem* **70:** 1366–1375.

DiGiuseppe JA, Weng LJ, Yu KH, Fu S, Kastan MB, Samid D, Gore SD (1999). Phenylbutyrate-induced G1 arrest and apoptosis in myeloid leukemia cells: Structure-function analysis. *Leukemia* **13:** 1243–1253.

Dringen R, Pfeiffer B, Hamprecht B (1999). Synthesis of the antioxidant glutathione in neurons: Supply by astrocytes of CysGly as precursor for neuronal glutathione. *J Neurosci* **19:** 562–569.

Escher P, Wahli W (2000). Peroxisome proliferator-activated receptors: Insight into multiple cellular functions. *Mutat Res* **448:** 121–138.

Forman BM, Tontonoz P, Chen J, Brun RP, Spiegelman BM, Evans RM (1995). 15-Deoxy-delta 12, 14-prostaglandin J2 is a ligand for the adipocyte determination factor PPAR gamma. *Cell* **83:** 803–812.

Gelman L, Fruchart JC, Auwerx J (1999). An update on the mechanisms of action of the peroxisome proliferator-activated receptors (PPARs) and their roles in inflammation and cancer. *Cell Mol Life Sci* **55:** 932–943.

Goodwin CJ, Holt SJ, Downes S, Marshall NJ (1995). Microculture tetrazolium assays: A comparison between two new tetrazolium salts, XTT and MTS. *J Immunol Methods* **179:** 95–103.

Hacki J, Egger L, Monney L, Conus S, Rosse T, Fellay I, Borner C (2000). Apoptotic crosstalk between the endoplasmic reticulum and mitochondria controlled by Bcl-2. *Oncogene* **19:** 2286–2295.

Handler JA, Seed CB, Bradford BU, Thurman RG (1992). Induction of peroxisomes by treatment with perfluorooctanoate does not increase rates of H_2O_2 production in intact liver. *Toxicol Lett* **60:** 61–68.

Inoue I, Noji S, Awata T, Takahashi K, Nakajima T, Sonoda M, Komoda T, Katayama S (1998). Bezafibrate has an antioxidant effect: Peroxisome proliferator-activated receptor alpha is associated with Cu^{2+}, Zn^{2+}-superoxide dismutase in the liver. *Life Sci* **63:** 135–144.

Johnson TE, Holloway MK, Vogel R, Rutledge SJ, Perkins JJ, Rodan GA, Schmidt A (1997). Structural requirements and cell-type specificity for ligand activation of peroxisome proliferator-activated receptors. *J Steroid Biochem Mol Biol* **63:** 1–8.

Kim HT, Qiang W, Wong PK, Stoica G (2001). Enhanced proteolysis of IκBα and IκBβ proteins in astrocytes by Moloney murine leukemia virus (MoMuLV)-ts1 infection: A potential mechanism of NF-kappa*B* activation. *J NeuroVirol* **7:** 466–475.

Kliewer SA, Umesono K, Mangelsdorf DJ, Evans RM (1992). Retinoid X receptor interacts with nuclear receptors in retinoic acid, thyroid hormone and vitamin D3 signalling. *Nature* **355:** 446–449.

Lin YC, Chow CW, Yuen PH, Lynn WS, Wong PKY (1997). Establishment and characterization of conditionally immortalized astrocytes to study their interaction with *ts*1, a neuropathogenic mutant of Moloney murine leukemia virus. *Neuro Virol* **3:** 28–37.

Miele M, Boutelle MG, Fillenz M (1994). The physiologically induced release of ascorbate in rat brain is dependent on impulse traffic, calcium influx and glutamate uptake. *Neurosci* **62:** 87–91.

Mollace V, Nottet HS, Clayette P, Turco MC, Muscoli C, Salvemini D, Perno CF (2001). Oxidative stress and neuroAIDS: Triggers, modulators and novel antioxidants. *Trends Neurosci* **24:** 411–416.

Muga SJ, Thuillier P, Pavone A, Rundhaug JE, Boeglin WE, Jisaka M, Brash AR, Fischer SM (2000). 8S-lipoxygenase products activate peroxisome proliferator-activated receptor alpha and induce differentiation in murine keratinocytes. *Cell Growth Differ* **11:** 447–454.

Pace GW, Leaf CD (1995). The role of oxidative stress in HIV disease. *Free Radic Biol Med* **19:** 523–528.

Pahl HL, Baeuerle PA (1997). The ER-overload response: Activation of NF-κB. *Trends Biochem Sci* **22:** 63–67.

Poynter ME, Daynes RA (1998). Peroxisome proliferator-activated receptor alpha activation modulates cellular redox status, represses nuclear factor-κB signaling, and reduces inflammatory cytokine production in aging. *J Biol Chem* **273:** 32833–32841.

Reddy JK, Goel SK, Nemali MR, Carrino JJ, Laffler TG, Reddy MK, Sperbeck SJ, Osumi T, Hashimoto T, Lalwani ND, Rao MS (1986). Transcription regulation of peroxisomal fatty acyl-CoA oxidase and enoyl-CoA hydratase/3-hydroxyacyl-Co A dehydrogenase in rat liver by peroxisome proliferators. *Proc Natl Acad Sci USA* **83:** 1747–1751.

Rizzuto R, Pinton P, Carrington W, Fay FS, Fogarty KE, Lifshitz LM, Tuft RA, Pozzan T (1998). Close contacts with the endoplasmic reticulum as determinants of mitochondrial Ca^{2+} responses. *Science* **280:** 1763–1766.

Samid D, Shack S, Myers CE (1993). Selective growth arrest and phenotypic reversion of prostate cancer cells *in vitro* by nontoxic pharmacological concentrations of phenylacetate. *J Clin Invest* **91:** 2288–2295.

Samid D, Wells M, Greene ME, Shen W, Palmer CN, Thibault A (2000). Peroxisome proliferator-activated receptor gamma as a novel target in cancer therapy: Binding and activation by an aromatic fatty acid with clinical antitumor activity. *Clin Cancer Res* **6:** 933–941.

Shikova E, Lin Y-C, Saha K, Brooks BR, Wong PKY (1993). Astrocyte-specific defective $gPr80^{env}$ processing correlates with cytopathogenicity induced by *ts*1, a mutant of Moloney murine leukemia virus. *J Virol* **67:** 1137–1147.

Soliman MS, Cunningham ML, Morrow JD, Roberts LJ, Badr MZ (1997). Evidence against peroxisome proliferation-induced hepatic oxidative damage. *Biochem Pharmacol* **53:** 1369–1374.

Stoica G, Illanes O, Tasca S, Wong PKY (1993). Temporal central and peripheral nervous system changes induced by a paralytogenic mutant of Moloney murine leukemia virus TB. *Lab Invest* **66:** 427–436.

Stoica G, Tasca SI, Wong PK (2000). Motor neuronal loss and neurofilament-ubiquitin alteration in MoMuLV-ts1

encephalopathy. *Acta Neuropathol (Berl)* **99:** 238–244.

Takeshima T, Johnston JM, Commissiong JW (1994). Mesencephalic type 1 astrocytes rescue dopaminergic neurons from death induced by serum deprivation. *J Neurosci* **14:** 4769–4779.

Thuillier P, Anchiraico GJ, Nickel KP, Maldve RE, Gimenez-Conti I, Muga SJ, Liu KL, Fischer SM, Belury MA (2000). Activators of peroxisome proliferator-activated receptor-alpha partially inhibit mouse skin tumor promotion. *Mol Carcinog* **29:** 134–142.

Thuillier P, Baillie R, Sha X, Clarke SD (1998). Cytosolic and nuclear distribution of PPARgamma2 in differentiating 3T3-L1 preadipocytes. *J Lipid Res* **39:** 2329–2338.

Ullian EM, Sapperstein SK, Christopherson KS, Barres BA (2001). Control of synapse number by Glia. *Science* **291:** 657–661.

Wong PKY, Lynn WS, Lin YC, Choe W, Yuen PH (1998). *ts*1 MoMuLV: A murine model of neuroimmunodegeneration. In *Neuroimmunodegeneration*, Wong PKY, Lynn WS (eds). RG Landes: Heidelberg, pp 75–93.

Yeldandi AV, Rao MS, Reddy JK (2000). Hydrogen peroxide generation in peroxisome proliferator-induced oncogenesis. *Mutat Res* **448:** 159–177.